

Thick-Film Thermistor Array Using a Novel Threshold Conversion Concept

Terence C. W. Yeow¹, Malcolm R. Haskard¹, Dennis E. Mulcahy²,
Hwa-Il Seo³ and Stanley H. H. Lim¹

¹Microelectronics Centre, University of South Australia

²Analysis and Sensors Group, School of Chemical Technology, University of South Australia
P. O. Box 1, Ingle Farm SA 5098, Australia

³Department of Electronics, Korea Institute of Technology & Education,
Chungnam 333-860, Korea

(Received February 13, 1996; accepted October 31, 1997)

Key words: thick-film, sensor arrays, threshold conversion, temperature

Growing interest in the mimicking of human sensory systems has spurred us to investigate a simple but effective method of processing very large sensor array signals. In this paper we describe the novel concept of threshold conversion as applied to a large array of 256 thick-film thermistors. The results show that threshold conversion is a viable and effective method of processing large sensor array data, making it possible for large sensor arrays to be utilized without the disadvantages of complex circuitry and long measurement time.

1. Introduction

1.1 *Threshold conversion concept*

There is growing interest among research groups in the production of systems that mimic human sensory mechanisms.⁽¹⁻⁴⁾ Examples are vision, smell, touch and taste. All human sensory systems utilize very large sensor arrays. For example, the tongue typically has several thousand taste buds, the olfactory system consists of a million or more sensors and in these two examples mixtures of groups of similar or dissimilar sensors are involved.

Consequently, in order to successfully mimic human sensory systems, very large sensor arrays with simple and effective control and processing methods are needed. We present here an array processing method based upon the novel concept of threshold conversion on a thick-film thermistor array.

In 1992, a novel strategy of using an array of sensors with built-in thresholds so that sensors switch at different input levels was proposed.⁽⁴⁾ If a particular sensor had an built-in threshold, then it would produce an active high output only when the input signal exceeded or equalled the built-in threshold value, as shown below:

$$V_{in} < V_{th}, \text{ then } V_{out} = 0$$

$$V_{in} \geq V_{th}, \text{ then } V_{out} = 1,$$

where V_{th} is the built-in threshold voltage.

This strategy could be used in an array of analog sensor cells that act collectively as an area sensor. It would act as a simple analog-to-digital converter for the array, and thereby eliminate the need for precise and complex circuitry to accommodate analog signals. However, in order to fully utilize the threshold conversion technique, each sensor cell would require a different built-in threshold. The individual sensors would then switch at different input levels. A range of threshold values must be used which cover the full range of the measured input signal. A simple descriptive representation of the operation of the built-in threshold conversion scheme used in a 4×4 array of temperature sensors is shown in Fig. 1.

In this example, each temperature sensor is assigned a linearly increasing built-in threshold voltage. This is performed by first calibrating the temperature sensors by

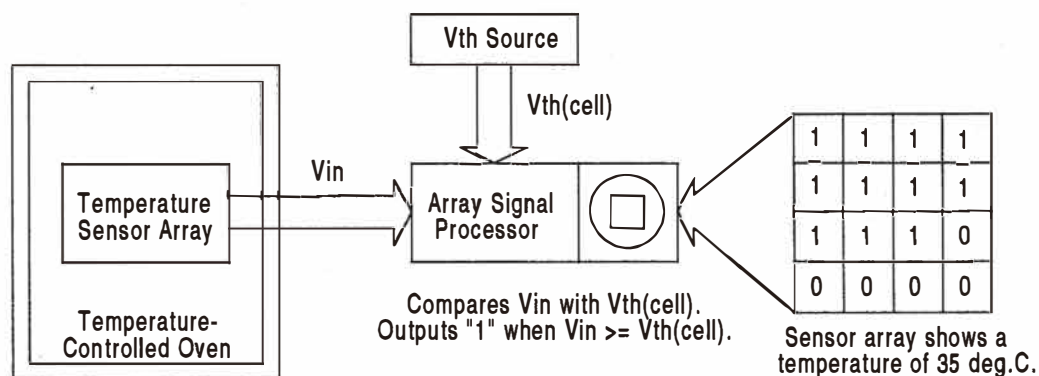


Fig. 1. Simple description of 4×4 temperature sensor array using threshold conversion.

recording their output voltages from 25°C to 40°C in 1°C steps. Each sensor is then assigned a built-in threshold voltage, V_{th} (cell), that represents one of these temperature steps. Hence, each sensor will only produce an active high output when the measured temperature is equal to or higher than the temperature value assigned to that particular sensor. In other words, the number of active high outputs from the array would indicate the measured temperature. For a temperature of 35°C, the number of active high outputs from the sensor array would be 11, as shown in Fig. 1.

Two features that a sensor array using this threshold conversion technique must possess before it can be used successfully are, firstly, that a large number of sensors be used in the array since the number of sensors closely corresponds to the sensor's accuracy, resolution and measurement range. In general, the larger the array size, the better these characteristics. Secondly, the sensor structures should be small and simple, allowing high packing densities to keep the sensor size small. Microelectronic technology has allowed the fabrication of small, simple sensors, such as ion-sensitive field-effect transistors (ISFETs)⁽⁵⁾ and capacitive/conductive sensors. In addition to the simplicity of this concept, all the advantages of utilizing a sensor array would be obtained such as improved reliability due to redundancy and improved accuracy due to statistical treatment of the measured signals.

1.2 Threshold conversion schemes

The concept of threshold conversion is simple, and there are numerous schemes whereby it could be implemented. In this paper, we propose four major schemes and three minor schemes that utilize combinations of the major ones. They are listed below.

Scheme 1: Linearly increasing V_{th} for each sensor cell at every array scan

This scheme was introduced in the earlier section as a simple example. Every cell in the sensor array is assigned a linearly increasing V_{th} , so that a measurement covering the desired measurement range can be performed in a single scan of the array. As shown in the example, the first and last sensor cells in the array are assigned a V_{th} corresponding to the lower and upper limits of the sensor's measurement range, respectively. The advantages of this conversion scheme are fast measurement since the full measurement range can be covered with one complete scan of the sensor array, and high reliability due to the self-checking nature of the scheme. That is, erroneous cells could be omitted from consideration by comparing the known output with the measured signal. However, one disadvantage is that resolution and measurement range are limited by the size of the sensor array. If a higher resolution were required, then the measurement range should be decreased for the same number of cells. Thus, for a fixed number of sensor cells, if the resolution is increased, the V_{in} range decreases.

Scheme 2: Same V_{th} for all sensor cells, but linearly increased at next array scan

This scheme designates the same V_{th} for all cells in the array but it is then linearly increased at the next array scan. As in the previous scheme, the sensor array must be calibrated in the first instance and the lower and upper V_{th} range must be defined. Measurements are then made by scanning every sensor cell in the array with the same V_{th} , but linearly increasing it at the next array scan, moving from the lower to the upper V_{th}

range. This method differs in that the complete measurement process takes longer as each cell is scanned n^2 times, where n is the number of cells in the array. Hence, instead of adding up the number of "1"s from the whole array, this method adds up the total number of "1"s from each array scan. The advantages of this scheme are high reliability due to redundancy, and high accuracy due to statistical application of the V_{th} conversion scheme where multiscanning of the array cells is performed. The disadvantages of this scheme are slow measurement, since it requires " n^2 " array scans to cover the full measurement range of "0 to n " V_{th} for n cells in the array, poor resolution and limited measurement range.

Scheme 3: Randomly selected V_{th} for each sensor cell which is fixed for every array scan

The user input threshold voltage, V_{th} , for this scheme is selected at random anywhere between the lower and upper V_{th} values which were obtained from sensor calibration prior to measurements. This randomly selected V_{th} value is then assigned to a sensor cell such that each cell has a randomly selected V_{th} value. This V_{th} designation to each cell in the array is then used for every array scan. Thus, a look-up table (LUT) could be made to facilitate comparison of the sensor output signal with the desired V_{th} value. The advantage of using this conversion scheme is fast measurement, needing only one complete scan to cover the full measurement range. The disadvantage of this scheme is the limitation of sensor accuracy due to array size. In order to achieve high accuracy, a large number of sensor cells are needed. As an example, an array consisting of 1000 sensors will have an accuracy better than 5%, using the 5 and 95 percentiles of the output range.⁽⁴⁾

Scheme 4: Same V_{th} for all sensor cells, but randomly selected at every array scan

This conversion scheme is a combination of schemes (2) and (3). After the lower and upper V_{th} limits have been determined via initial sensor calibration, all sensor cells in the array are assigned the same randomly selected V_{th} value. This V_{th} value is randomly selected again after the completion of each array scan. As in scheme (2), each cell in an n -cell array is multiscanned n^2 times to obtain a grand total of the number of cells activated. The advantages of using this conversion scheme are high reliability due to redundancy and high accuracy due to statistical application of the V_{th} conversion scheme to the array signals via multiscanning techniques. The disadvantages are slow measurement due to the multiscanning methodology and limitation of resolution and measurement range by virtue of the long measurement time.

Scheme 5: Randomly selected V_{th} for each sensor cell at every array scan

This scheme is similar to scheme (4) but with the designated V_{th} for each cell in the array selected randomly at every array scan. Hence the V_{th} value for the whole array is dynamically changing all the time. The advantages of this conversion scheme are high reliability due to redundancy and fast measurement since one complete measurement may be made in one array scan. The disadvantage is that sensor accuracy is limited by the size of the array. Thus, to achieve high accuracy, a large number of sensor cells are needed.

Scheme 6: Randomly selected V_{th} for each randomly selected sensor cell at every array scan

A random selection of sensor cells is made from the sensor array and each of them is assigned a V_{th} value, also randomly selected. This process is repeated at the next array scan. Hence, random sections of the sensor array are repeatedly selected and assigned a random V_{th} value for each of the cells selected. The measurement time is greatly increased using this scheme as only small sections of the sensor array are accessed at any one array scan. However, due to the small number of cells selected, the reliability and accuracy of the sensor may be impaired. If the number of cells selected were increased, this scheme would be identical to scheme (5).

Scheme 7: Same V_{th} for all randomly selected sensor cells and randomly selected at every array scan

A random selection of sensor cells is made from the sensor array and they are assigned a randomly selected V_{th} value. This process is repeated at the next array scan. Hence, random sections of the sensor array are repeatedly selected and assigned a random V_{th} value for all of the cells selected. This is similar to scheme (4). A V_{th} LUT and an initial sensor calibration are required. The measurement time using this scheme is quite short; however, it depends on the number of cells accessed. If all the cells in the array were accessed, then it would be exactly the same as for scheme (4). The disadvantages of this scheme are poor reliability and accuracy if the number of cells scanned is too small.

2. Experimental

2.1 Thermistor array construction

The sensor array was designed using a thick-film hybrid design CAD tool called CAHL (Computer Aided Hybrid Layout, University of South Australia). A 20×19 array matrix of thick-film thermistors was designed, as shown in Fig. 2. However, only 16×16 sensors for a total of 256 thermistors were used. Each thermistor had dimensions of $0.8 \text{ mm} \times 0.8 \text{ mm}$. The dielectric crossover was $1.2 \text{ mm} \times 1.2 \text{ mm}$ and the conductor track was 0.5 mm wide. The thick-film pastes used were thermistor paste NTC 2414 (ESL, Penn., USA) with a sheet resistivity of $10 \text{ k}\Omega/\text{sq}$, conductor paste ESL 9502 (ESL, Penn., USA) and dielectric paste 8190 (Dupont Co, Wilmington, Delaware, USA). The sensors were printed on alumina substrates of $76 \text{ mm} \times 76 \text{ mm}$ size and dried at 100°C for 15 min before firing at 850°C for 50 min.

2.2 Measurement setup

The experimental setup is shown in Fig. 3. It included the thermistor array and control circuit, dc power supply, Philips inter-integrated circuit (IIC, Philips Co. Pty. Ltd., NSW, Australia) bus-PC interface card, IBM compatible PC (386DX33), k-type thermocouple (Model 820, Tegam Inc.) and temperature-controlled oven (Laboro, Selby Pty. Ltd. Co.) with a temperature controller fabricated by us. The control circuit consisted of two analog multiplexers (MC14067), an 8-bit IIC A/D converter (PCF8591) and two IIC I/O expanders (PCF8574). IIC compatible IC chips were chosen since they gave improved perfor-

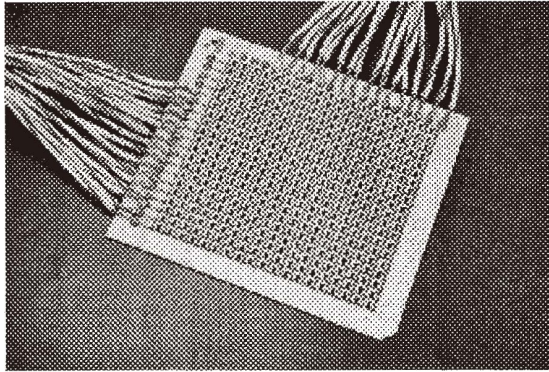


Fig. 2. Photograph of thick-film thermistor sensor array.

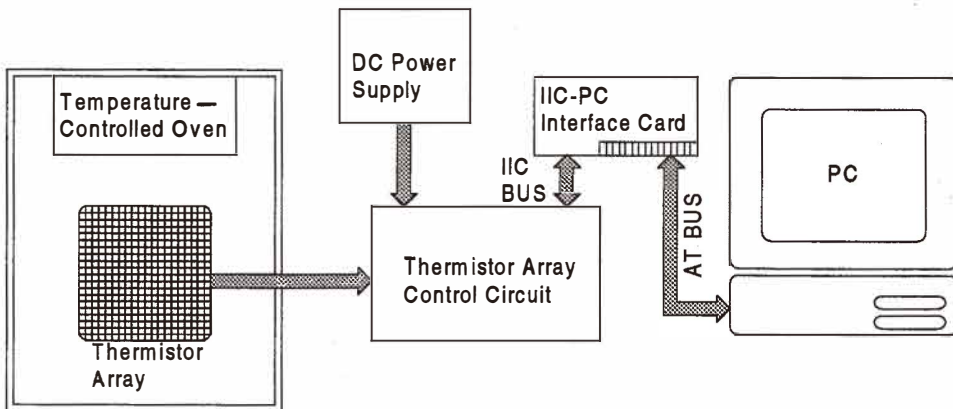


Fig. 3. Thermistor array experimental setup.

mance over conventional RS232 chips. An “expert system” shell called CRYSTAL V4.0 was used to control the thermistor array via the IIC bus. The thermistor array was placed in the temperature-controlled oven at room temperature and measurements taken at intervals of 5°C from 25°C to 95°C. A 30-min settling time was allowed at each change in temperature before measurements were taken. All measurements were saved on disk for later processing with the V_{th} conversion program.

2.3 Threshold conversion program

The V_{th} conversion program was written using Microsoft Basic Professional Version 7.0 (Microsoft Co., Redmond, USA). The functions of this program were to read the output signal voltages of the thermistor array saved on disk and to perform appropriate V_{th} conversions. All seven V_{th} conversion schemes were included. Other supplementary programs were also written to aid the processing of the array data. The flow chart of the V_{th} conversion processing program is shown in Fig. 4.

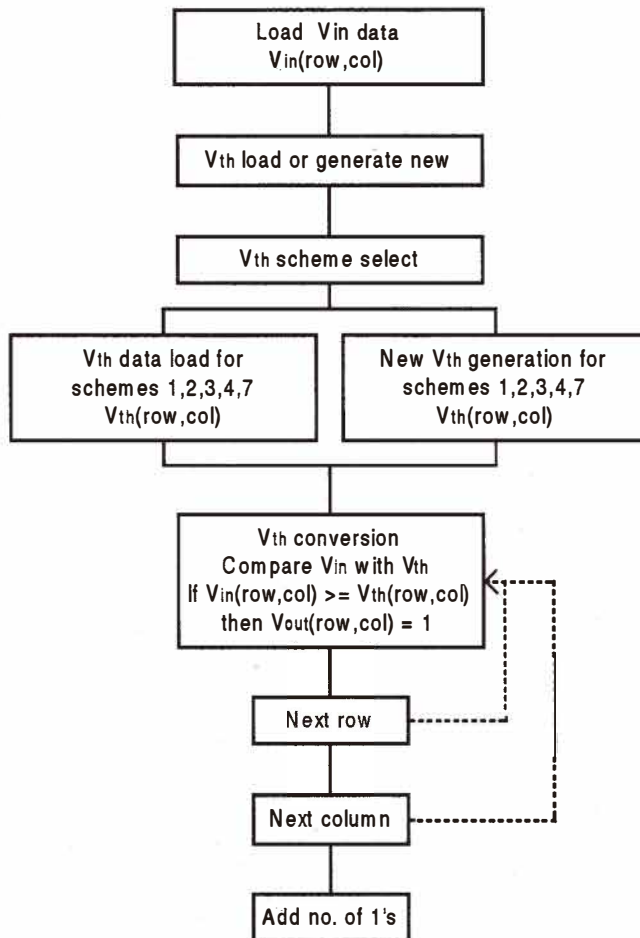


Fig. 4. Flow chart of V_{th} conversion processing program.

3. Results and Discussion

3.1 Calibration

A calibration curve for the thermistor array from 25°C to 95°C at 5°C intervals was constructed as a basis for comparison of the subsequent V_{th} conversion processing. This calibration curve is shown in Fig. 5(a). The voltage output from each thermistor in the array, designated V_{in} , was converted using seven different V_{th} conversion schemes to obtain a set of V_{th} conversion calibration curves as shown in Figs. 5(b) to 5(j). V_{th} conversion schemes (6) and (7) each had options of 64 cells and 144 cells. The notation “ n ” indicates the number of cells activated (or cells displaying an active high digital level), “ nt ” indicates the total number of cells activated for multi-scanned V_{th} conversion schemes, and “ N ” indicates the normalized value of either “ n ” or “ nt ”.

The V_{in} calibration curve shown in Fig. 5(a) has a slope of 34.1 mV/°C. The V_{th} conversion calibration curves for all seven schemes show good correlation with the thermistor's V_{in} calibration curve, with regression slopes ranging from 45 to 54.9 mV/°C. This range is higher than the value from the V_{in} calibration graph (34.1 mV/°C). However, it is acceptable since a direct comparison between V_{in} and “ n ” or “ nt ” could not be made. The most important factor is that the calibration curves are linear, with the exception of those for schemes (5) and (6). These schemes show poor linearity compared with the other schemes because they use a random V_{th} value for each cell in the array at each array scan. Hence it can be deduced that as the number of cells decreases, nonlinearity increases, as shown in Figs. 5(f) to 5(h).

3.2 Voltage spread

A study to determine the voltage spread of the thermistor cells in the array was carried out and yielded interesting results which are shown in Fig. 6. V_{in} spreads at 34.83°C, 53.1°C, 63°C, 82.38°C and 92.58°C were plotted against V_{in} . It can be seen from the figure that the V_{in} spread is larger at lower temperatures than at higher temperatures. This trend in the V_{in} spread is expected and conforms with theory.^(6,7) At low temperatures, the stability of the thermistor cells is poor and this brings about a large V_{in} spread.

3.3 Array output map

The thermistor array V_{th} converted output maps at 58°C for schemes (1) to (4) are shown in Fig. 7. The results for the linear V_{th} conversion method (scheme 1) do not strictly follow a linear cell activation trend. We expected to see a distinct division between the activated thermistor cells and the nonactivated ones. However, due to the V_{in} spread near or at the border of this change, no distinct division could be observed. This may be a problem when one tries to achieve accurate measurement at very small temperature changes. To overcome this problem, the multi-scan linear method (scheme 2) is employed. Here the array output map shows a gradual change at the border and hence would produce more accurate measurement. Random schemes (schemes 3, 4, 5, 7) do not suffer from these border uncertainties.

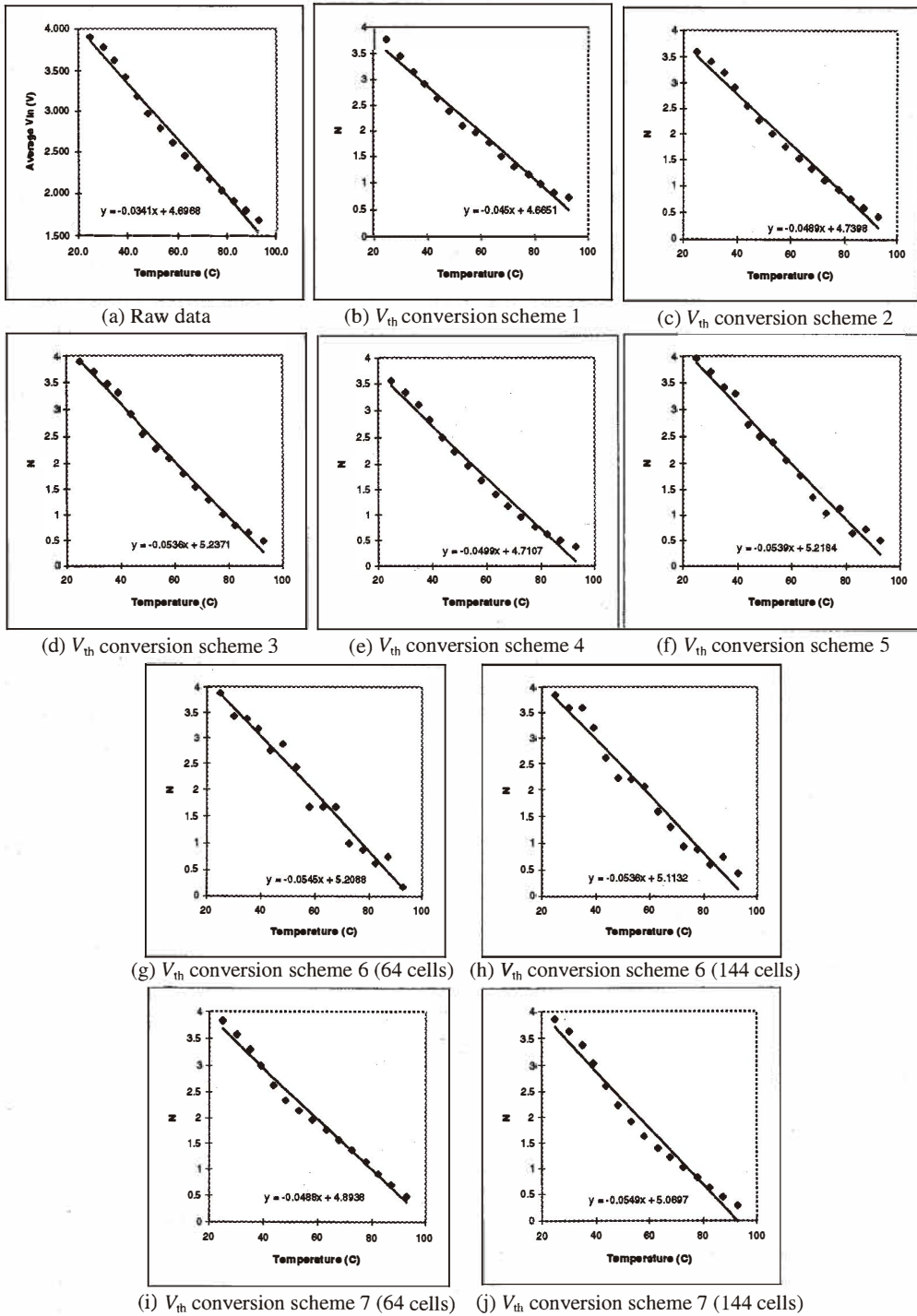
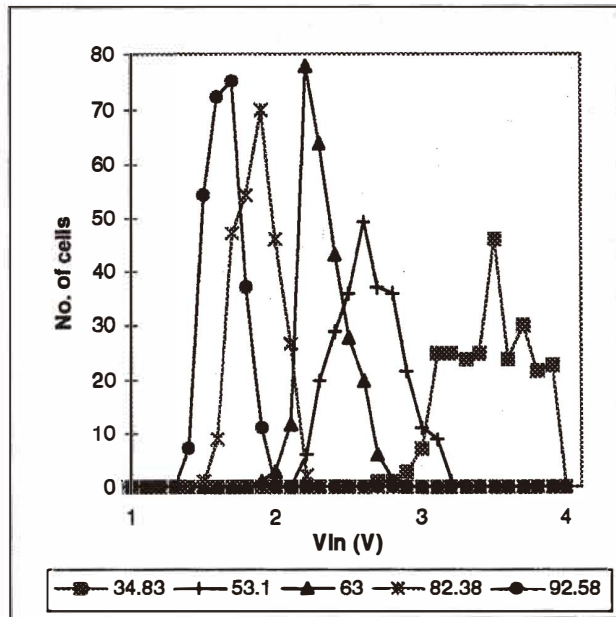


Fig. 5. V_{th} conversion calibration curves (N represents the normalized value of the total number of cell output "1", for single and multiple scanned conversion schemes).

Fig. 6. V_{in} spread.

3.4 Reliability

The reliability of the thermistor array measurement using various V_{th} conversion schemes was determined by inserting known errors (1% and 5%) into the V_{in} data file. Errors were inserted by giving V_{in} a "0" value, indicating that the cell is not working. Since differences between the calibration graphs for all three degrees of errors are small, the slopes of the calibration regression equations are compared with the error-free slope. This will be used to distinguish the V_{th} conversion schemes in order to determine the most reliable method. The results are shown in Table 1. It can be deduced from Table 1 that all the multiscanned schemes (schemes 2, 4 and 7) show good reliability, with random V_{th} and random cell scheme (scheme 5) being the best. This is due to its randomness and to the large number of cells involved. The reliability of scheme (6) is poor due to the small number of cells used in the array. If a multiscan method is used, as in scheme (7), a better reliability score is obtained.

3.5 Sensitivity

The sensitivity of the V_{th} conversion schemes is very important. It was evaluated by measuring very small temperature changes between 59.1°C and 58.9°C in steps of 0.1°C. A temperature near 60°C was chosen since that region has an average V_{in} spread (approximately 1.0 V). The V_{th} conversion results of the various schemes with the small temperature changes are shown in Fig. 8. The expected trend for the sensitivity graphs in Fig. 8 is

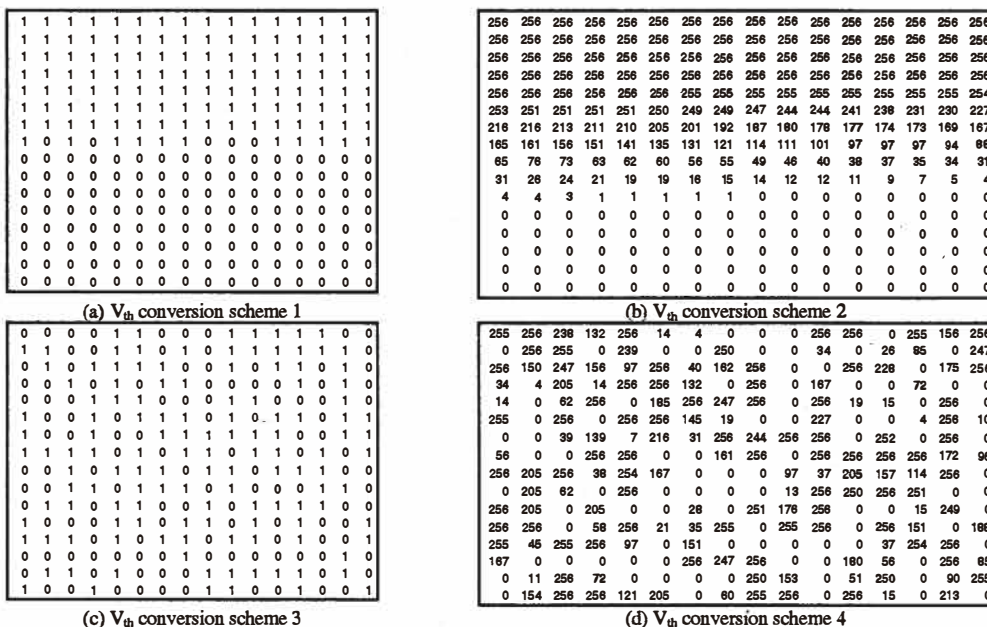
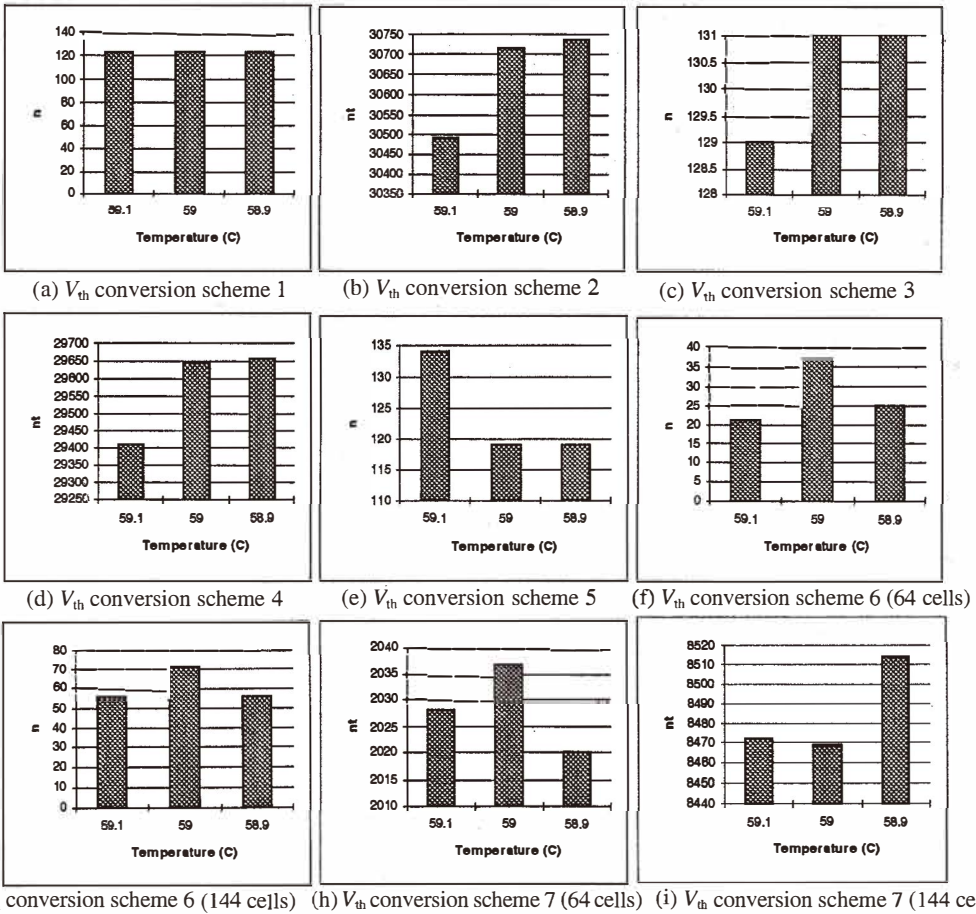


Fig. 7. Thermistor array V_{th} converted output maps at 58°C. (Note that the multiscanned schemes (schemes 2 and 4) show the total number of cells activated, “ nt ”.)

Table 1
Variations in slope with error-free data for various V_{th} conversion schemes.

V_{th} conversion scheme	Difference in slope for 1% error data	Difference in slope for 5% error data
1	0.889%	4.444%
2	0.818%	4.294%
3	0.559%	4.291%
4	0.802%	4.409%
5	0.371%	3.154%
6 (64 cells)	1.468%	10.826%
6 (144 cells)	3.178%	10.280%
7 (64 cells)	0.819%	4.303%
7 (144 cells)	0.546%	4.189%

Fig. 8. Sensitivity of V_{th} conversion schemes.

that as the temperature decreases the voltage output from the thermistor increases. This in turn increases the number of cells activated. Multiscanned schemes (schemes 2, 4 and 7) show large changes compared with the non-multiscanned schemes. The latter (schemes 1 and 3) show very little sensitivity to small temperature changes. This is probably due to the V_{in} spread at that particular temperature. The V_{in} spread study results in Fig. 6 show that the spread is larger at lower temperatures. The array output map shown in Fig. 7 for scheme (1) in particular shows that no distinct boundary between the activated and nonactivated cells is obtained. This would make resolution of very small temperature changes extremely difficult. However, the random scheme (3) shows better sensitivity since a random or an undefined boundary is present. Schemes (5) and (6) on the other hand show haphazard

changes as revealed in Fig. 8, indicating that these schemes are not suitable for sensitive measurements.

4. Conclusions

A full summary of the performance of various V_{th} conversion schemes in terms of processing thermistor array signals and presenting a reliable and accurate representation of the measured temperature is shown in Table 2. The best scheme suitable for the thermistor array depends on the particular application. Applications may require the thermistor array to have very good reliability, to be highly sensitive to small temperature changes, to have very fast response, or to have a combination of all or some of these features. In general, multiscanned schemes (schemes 2 and 4) have slower response since they require longer measurement times. However, an exception is scheme (7), where only one section of the array may be accessed, making it possible to reduce the measurement time. In general, schemes with randomly generated V_{th} show good reliability, with scheme (5) showing the best performance. Multiscanned schemes also show better sensitivity, as compared to single scanned schemes, to small temperature changes. A compromise scheme that shows good linearity, reliability, sensitivity and short measurement time would be scheme (7) with 64 cells accessed.

In this paper we have demonstrated that threshold conversion is a viable and innovative method of processing very large array signals. Various schemes have been proposed and tested on a thermistor array with some success. However, the thermistor array experiment is intended only as a general introduction to the potential of the threshold conversion concept. A more challenging application is implementation of the concept on a microelectrochemical sensor, namely a very large array of pH-ISFETs (ion-sensitive field-effect transistors).^(8,9) Here, it is expected that the threshold conversion scheme will bring us closer to true biological mimicry.

Table 2
Summary of performance of V_{th} conversion schemes.

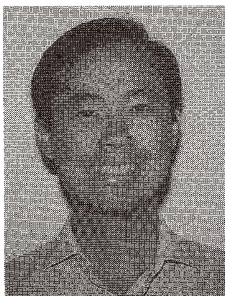
V_{th} conversion scheme	Slope (mV/°C)	Linearity	Reliability	Sensitivity
Raw	34.1	good	good	good
1	45	good	good	very good
2	48.9	good	good	good
3	53.6	good	good	poor
4	49.9	good	good	good
5	53.9	poor	very good	very poor
6 (64 cells)	54.5	very poor	poor	very poor
6 (144 cells)	53.6	very poor	poor	very poor
7 (64 cells)	48.8	good	good	good
7 (144 cells)	54.9	good	good	good

Acknowledgment

The authors would like to acknowledge the financial support from DEET provided by the Targeted Institutional Links grant.

References

- 1 K. Hayashi, M. Yamanaka, K. Toko and K. Yamafuji: Sensors and Actuators B **2** (1990) 205.
- 2 T. Nakamoto, A. Fukuda and T. Moriizumi: Sensors and Actuators B **10** (1993) 85.
- 3 J. W. Gardner, E. L. Hines and H. C. Tang: Sensors and Actuators B **9** (1992) 9.
- 4 M. R. Haskard and D. E. Mulcahy: Biosensors and Bioelectronics **7** 10 (1992) 689.
- 5 P. Bergveld: IEEE Trans. on Bio-medical Eng. **BME-17** (1970) 70.
- 6 M. R. Haskard: Thick Film Hybrids-Manufacture and Design (Prentice Hall, New York, 1988) Chap. 9.
- 7 M. L. Topfer: Thick Film Microelectronics-Fabrication, Design and Applications (Van Nostrand Reinhold Company, New York, 1971).
- 8 T. C. W. Yeow, D. E. Davey, H. L. Do, M. R. Haskard, D. E. Mulcahy and H. I. Seo: Proc. 13th Microelectronics Conference 1995 (IREE, Adelaide, 1995) p. 62.
- 9 T. Yeow, H. I. Seo, D. Mulcahy and M. Haskard: Journal of the Korean Sensors Society **4** 4 (1995) 55.

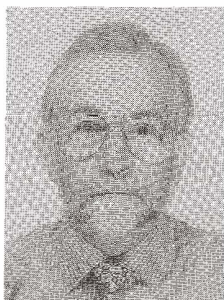


Terence C. W. Yeow received his B. Eng. and Ph.D. degrees in Electronic Engineering from the University of South Australia in 1992 and 1996, respectively. His Ph.D. work involved developing a very large ISFET sensor array chip for biosensor applications. Since 1996, he has been with the Australian Defence, Science and Technology Organization, Salisbury as a research scientist. His research interests include microelectronic chemical sensors and microengineered sensor systems.

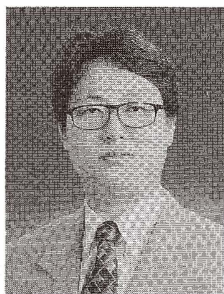


Malcolm R. Haskard was a Professor of Microelectronics, Head of the School of Electronic Engineering and Founding Director of the Microelectronics Centre at the University of South Australia. He retired late 1996 and now assists the University and Microelectronics Centre as an Adjunct Professor. His research interests include intelligent microelectronic sensors and microengineering. He has been an Australian Government adviser on microelectronics for the ASEAN region and on behalf of the University, the government and UNESCO has conducted many specialist courses in Australia and overseas. He was awarded significant funding to establish two Targeted Institutional Link Programs, covering both

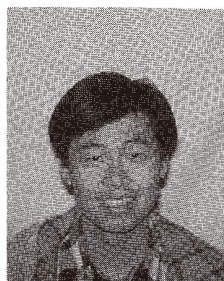
Universities and Government Research Establishments in South Korea and Indonesia. He is a Fellow of three Institutions, namely the Institution of Engineers (Australia), the Institution of Radio and Electronics Engineers (Australia) and the Institution of Electrical Engineers (London). He has published nine books and numerous papers in professional journals.



Associate Professor ***Dennis E. Mulcahy*** is Head of the School of Chemical Technology at the University of South Australia. He is also Education and Training Program Leader in the Cooperative Research Centre (CRC) for Water Quality and Treatment. He is author of 75 publications in physical chemistry, analytical chemistry and chemical education.



Hwa-II Seo was born in Korea in 1961 and received his Ph.D. degree in Electronic Engineering from Kyungpook National University, Korea in 1991. He was a Senior Researcher of the Sensor Technology Research Center in 1992–1993 and a visiting researcher in the Microelectronics Centre at the University of South Australia in 1995. Since 1993, he has joined the Department of Electronic Engineering, Korea Institute of Technology and Education as an Assistant Professor. His research interests include microelectronic chemical sensors and bioelectronic devices.



Stanley Hock Hin Lim received his B.S. degree in Electronic Engineering from University of South Australia, Adelaide, South Australia, Australia, in 1995. He is currently pursuing a Ph.D. degree in Information Technology at the same university. His research interests include adaptive signal processing, sensor arrays, and mobile and satellite communication systems.